

PHYSICAL PROPERTIES OF THE GIANT H II REGION G353.2+0.9 IN NGC 6357

JOAQUIN BOHIGAS¹, MAURICIO TAPIA¹, MIGUEL ROTH², AND MARIA TERESA RUIZ³

¹Instituto de Astronomía, UNAM, Apdo. Postal 877, 22800 Ensenada, B.C., México

E-mail: jbb@astrosen.unam.mx

²Las Campanas Observatory, Carnegie Institute of Washington, Casilla 601, La Serena, Chile

³Departamento de Astronomía, Universidad de Chile, Casilla 36-D, Santiago, Chile

(Received July 31, 2004; Accepted November 13, 2004)

ABSTRACT

Optical imaging and spectroscopy of G353.2+0.9, the brightest part of the giant H II region NGC 6357, shows that this H II region is optically thin, contains $\sim 300 M_{\odot}$ of ionized gas and is probably expanding into the surrounding medium. Its chemical composition is similar to that found in other H II regions at similar galactocentric distances if temperature fluctuations are significant. The inner regions are probably made of thin shells and filaments, whereas extended slabs of material, maybe shells seen edge-on, are found in the periphery. The radio continuum and H α emission maps are very similar, indicating that most of the optical nebula is not embedded in the denser regions traced by molecular gas and the presence of IR sources. About 10^{50} UV photons per second are required to produce the H β flux from the 11.3'x10' region surrounding the Pis 24 cluster that is south of G353.2+0.9. Most of the energy powering this region is produced by the O3-7 stars in Pis 24. Most of the 2MASS sources in the field with large infrared excesses are within G353.2+0.9, indicating that the most recent star forming process occurred within it. The formation of Pis 24 preceded and caused the formation of this new generation of stars and may be responsible for the present-day morphology of the entire NGC 6357 region.

Key words : ISM:H II regions –ISM:individual (NGC 6357)

I. INTRODUCTION

NGC 6357 contains several H II regions of different ages (Massi, Brand & Felli 1997). According to Chini & Krügel (1983), NGC 6357 is characterized by an abnormal reddening law. The brightest H II region in NGC 6357 at all wavelengths is G353.2+0.9. The sharp southern boundary of this region faces the massive open cluster Pis 24 (Pismis 1959), which contains a couple of the brightest and bluest stars known (stars N35 and N57), classified as O3.5If and O3.5III(f*) by Walborn et al. (2002). These stars produce more than enough energy to ionize and heat G353.2+0.9. For this reason the Pis 24 cluster is thought to be the exciting source of this region (*e.g.* Neckel 1978; Lortet, Testor & Niemela 1984; Massey, DeGioia-Eastwood & Waterhouse 2001). Massey et al. (2001) give a distance of 2.56 kpc to Pis 24.

There are several luminous near-infrared sources with *K*-band excesses embedded in the nebulosity (Persi et al. 1986). Some coincide with compact radiocontinuum VLA sources (Felli et al. 1990). Massi et al. (1997) found molecular gas located behind G353.2+0.9 or north of the sharp boundary facing Pis 24.

To further understand the properties of NGC 6357 we obtained an optical spectrum of its brightest H II re-

TABLE 1
DENSITY AND TEMPERATURE

Ratio	N_e (cm ⁻³)	
[S II]6717/6731	0.68	2460
[Cl III]5518/5538	1.09	1790
	T_e (°K)	
[N II](6548+6584)/5755	95.1	9700
[O III](4959+5007)/4363	272	9200

gion, G353.2+0.9. Taking full advantage of the brightness of G353.2+0.9 we also produced images of this region in several emission lines and inspected the bidimensional behaviour of several physical parameters. Finally, *JHK* images and photometry were retrieved from the All Sky Data Release of the *Two Micron All Sky Survey (2MASS)* image archive and catalog. These were supplemented by mid-infrared data from the *Mid-course Space Experiment (MSX)*. A full account of this work can be found in Bohigas et al. (2004). In this contribution we present our main results.

II. OPTICAL SPECTROSCOPY

Spectroscopy between 3650 and 7300 Å was obtained with the RC spectrograph at the 4 m telescope in

CTIO. The plate scale is $0.49''/\text{pix}$. The mean spectral resolution and dispersion are ~ 3 pixel and $1.21 \text{ \AA}/\text{pixel}$, respectively.

The effect of the abnormal reddening law (Chini & Krügel 1983) on the optical spectrum of G353.2+0.9 was considered. The relative strengths of the Balmer series lines were satisfactorily reproduced up to H ϵ using the standard extinction law (Seaton 1979, $R_V = 3.2$) and assuming $I(\text{H}\alpha)/I(\text{H}\beta) = 2.85$. With $R_V = 3.5$ (the abnormal extinction value) the unreddened relative line intensities at the blue end of the spectrum are up to $\sim 15\%$ smaller. Because of this a slightly smaller O^{+2} temperature (8800 vs. 9200 K) is found. The net result is that differences between the abundances derived from the abnormal and normal extinction laws are within the experimental errors. Thus, the entire analysis was made with Seaton's (1979) extinction law. Temperatures and densities of the region are given in Table 1. Abundances determined with and without temperature fluctuations are presented in Table 2.

Large beam observations of radio recombination lines yield temperatures between 6500 K from H109 α and 8100 K from H166 α and a mean environmental density of $\sim 20 \text{ cm}^{-3}$ (Azcarate, Cersosimo & Colomb 1987, who identify the region as RCW 131). Temperatures and densities in G353.2+0.9 are significantly larger (Table 1), which implies that the region is overpressurized and probably expanding.

Abundances in G353.2+0.9 can be compared to those found in the Lagoon Nebula (M 8), which is 6 kpc from the galactic center (NGC 6357 is 6.5 kpc away). Esteban et al. (1999) determined the chemical composition of M 8 using permitted lines (when available) and considering temperature fluctuations. With the exception of helium, abundances in M 8 are significantly larger than those in G353.2+0.9 when no temperature fluctuations are considered (Table 2). If we consider the effect of fluctuations, assuming $t^2 = 0.05$ and using equations (12) and (13) from Peimbert & Costero (1969), we find a much better agreement. It is worth noticing that the mid-infrared data furnished by Giveon et al. (2002) and their equations for the neon and argon abundances (equation 10), lead to $\text{Ne} \simeq 1.2 \times 10^{-4}$ and $\text{Ar} \simeq 3.3 \times 10^{-6}$, very close to those found when temperature fluctuations are considered. All these indicates that substantial temperature fluctuations may be present in G353.2+0.9.

III. OPTICAL IMAGING

Narrow-band images were obtained at Las Campanas Observatory using the 40 inch telescope (LCO-40). The plate scale is $0.69''/\text{pixel}$ and image quality was ~ 2 pixel (FWHM of stellar images) during the whole observing run. We took images of the region for the most intense emission lines, as well as their nearby continuum. These images were flux-calibrated using our spectral data. In Fig. 1 we show a bias and flat field-corrected image of the region in [S III]9069 \AA . The

TABLE 2
ABUNDANCES

Element	$t^2 = 0$	$t^2 = 0.05$
He	0.107	0.107
O $\times 10^{-4}$	2.48	5.31
N $\times 10^{-5}$	5.16	8.79
S $\times 10^{-6}$	6.32	11.3
Ne $\times 10^{-5}$	4.04	10.2
Ar $\times 10^{-6}$	2.31	4.32



Fig. 1.— Bias and flat field-corrected image of the region in [S III]9069 \AA . Larger fluxes are depicted in black. The field-of-view is $11.3' \times 10'$. North is up, east is to the left.

field-of-view is $11.3' \times 10'$. The image is nearly centered on the brightest stars in the Pis4 cluster.

A $C(\text{H}\beta)$ image was produced from the $\text{H}\alpha/\text{H}\beta$ image assuming that this ratio is equal to 2.85 throughout the region and using Seaton's (1979) extinction law. Extinction is usually larger in the brightest regions. The flux-calibrated $\text{H}\beta$ image was dereddened using the $C(\text{H}\beta)$ frame, and we find that the extinction corrected $\text{H}\beta$ flux is $I(\text{H}\beta) \simeq 5 \times 10^{-8} \text{ erg cm}^{-2} \text{ s}^{-1}$. This result is consistent with other measurements (eg Felli et al. 1990; Copetti 2000). About 8×10^{49} ionizing photons per second are required to produce this flux at a distance of 2.56 kpc. The rate of UV photons produced by the two earliest-type stars in the Pis 24 cluster (N35 and N57) is $\sim 2 \times 10^{50}$ (Vacca et al. 1996), more than enough to maintain the ionization of G353.2+0.9 and the surrounding gas.

An electron density (N_e) map was obtained from the continuum-subtracted [S II]6724 \AA over [S II]6731 \AA image ratio using the following fit (Pérez-Tijerina, E., pri-

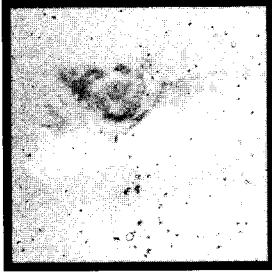


Fig. 2.— [N II]6584/H α image. Continuum was subtracted from the [N II]6584 Å and H α frames. The field-of-view is 6' \times 6'. North is up, east is to the left. Larger ratios are depicted in black.

vate communication):

$$\frac{I([\text{S II}]6717)}{I([\text{S II}]6731)} = 0.444 + \frac{0.988}{1 + \exp[\ln N_e - 6.658]} \quad (1)$$

The map was limited to those regions with a significantly large signal-to-noise ratio. The mass of ionized hydrogen was derived from the H β intensity and the electron density maps using the following formula.

$$M(\text{H}^+) = \frac{4\pi D^2 m_H I(\text{H}\beta)}{E_{42} < N_e >} \quad (2)$$

where D is the distance to the object, m_H is the hydrogen atom mass, $I(\text{H}\beta)$ is the extinction-corrected H β flux, E_{42} is the weakly temperature-dependent effective recombination emissivity and $< N_e >$ is the mean electron density. In the region included in the density map the mass of ionized hydrogen is close to $290 M_\odot$. From the remaining reddening-corrected H β flux emerging from the entire $11.3' \times 10'$ field, we estimate an additional H^+ mass close to $2 \times 10^5 / < N_e > M_\odot$, where $< N_e >$ is the mean electron density in the region surrounding G353.2+0.9. If $< N_e > = 20 \text{ cm}^{-3}$ (Azcárate et al. 1987), the mass of ionized hydrogen in the $11.3' \times 10'$ field centered at and including G353.2+0.9 is close $10^4 M_\odot$.

The extension of the emitting region along the line of sight, defined by the parameter l , can be estimated from

$$l = \frac{I(\text{H}\beta)}{4\pi E_{42} < N_e >^2 \tan^2 \theta} \quad (3)$$

where θ is the field-of-view of a pixel ($0.69''$). Uncertainties in this parameter are large since it depends on the square of the density. The largest depths of the emitting gas are found in the southern and southwestern edge, where $l \sim 1 - 5 \text{ pc}$. On the contrary, in the innermost parts of the nebula and in the bright extended filaments, $l \sim 10^{-3} \text{ pc}$. These numbers may

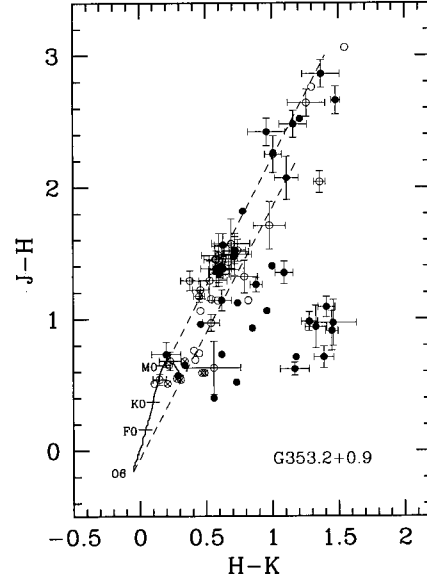


Fig. 3.— $H - K$ vs. $J - H$ diagram of near-infrared sources within the limits of G353.2+0.9 (filled circles) and those between this region and the Pis 24 star cluster (open symbols). Circles with a cross are optically bright OB-type stars in Pis 24. The continuous line marks the locus of main sequence (Koornneef 1983). The two parallel dashed lines represent the standard reddening vectors for late and early-type stars; their length corresponds to $A_V = 20$.

be incorrect by a factor of 10 or maybe more, but the large difference is probably real, and it indicates that the inner regions of the nebula are either filaments or thin shells, whereas extended slabs of material, possibly shells seen edge-on, are seen in the periphery.

In Fig. 2 we present a [N II]6584/H α image of the region. As can be seen, the nitrogen lines are clearly more intense away from the exciting stars (larger ratios, depicted in black), showing that the side of the nebula facing the Pis 24 cluster is more highly excited. This is supported by an RGB image of the same region (not shown) with $R = [\text{S II}]6724 \text{ \AA}$, $G = \text{H}\alpha$ and $B = [\text{O III}]5007 \text{ \AA}$. This is an additional evidence that most of the energy powering this H II region is provided by this cluster. Most of the material in the region between the cluster and G353.2+0.9 has been swept-up by stellar winds, which accounts for the very faint emission in this direction.

IV. INFRARED PHOTOMETRY

In Fig. 3 we present an $H - K$ vs. $J - H$ diagram of near-infrared sources in the region (all data from 2MASS). Notice that a large number of sources, all of them located within G353.2+0.9 (filled circles), have significant near-infrared excesses ($E(H - K) > 0.35$ assuming they are early-type stars). It can be shown from an H vs. $H - K$ that these are embedded B0-B5

main sequence stars. This shows that the most recent star formation region is located within G353.2+0.9. It is worth mentioning that the mid-infrared MSX image shows absolute and local maxima coinciding with the near-infrared point sources, a result that is interpreted as evidence that the dust grains are heated locally. In this context it is worth noticing that several of the small-scale features in the ionized gas distribution are closely related to the embedded near-infrared source population, which indicates that some local ionization also occurs within the nebula.

ACKNOWLEDGEMENTS

One of the authors (JB) is very grateful for the warm and excellent hospitality received from all our Korean hosts, in particular Seungsoo Hong and Jongsoo Kim. Partial support from DGAPA-UNAM projects IN-108696 and IN-105400 is acknowledged by JB and MT. MTR received partial support from FONDAPE (15010003) and Fondecyt grant number 1010404.

REFERENCES

- Azcárate, I.N., Cersosimo, J.C., & Colomb, F.R. 1987, *RevMexAA* 15, 3
- Bohigas, J., Tapia, M., Roth, M., & Ruiz, M.T. 2004, *AJ* 127, 2826
- Chini, R., & Krügel, E. 1983, *A&A* 117, 289
- Copetti, M.V.F. 2000 *A&AS* 147, 93
- Esteban, C., Peimbert, M., Torres-Peimbert, S., García-Rojas, J., & Rodríguez, M. 1999, *ApJS* 120, 113
- Felli, M., Persi, P., Roth, M., Tapia, M., Ferrari-Toniolo, M., & Cervelli, A. 1990, *A&A* 232, 477
- Giveon, U., Sternberg, A., Lutz, D., Feuchtgruber, H., & Pauldrach, A.W.A. 2002, *ApJ* 566, 880
- Koornneef 1983, *A&A* 128, 84
- Lortet, M.C., Testor, G., & Niemela, V. 1984, *A&A* 140, 24
- Massi, F., Brand, J., & Felli, M. 1997, *A&A* 320, 972
- Massey, P., DeGioia-Eastwood, K., & Waterhouse, E., 2001, *AJ* 121, 1050
- Neckel, T. 1978, *A&A* 68, 71
- Peimbert, M., & Costero, R. 1969, *Bol. Obs. Tonantzintla y Tacubaya* 5 3
- Persi, P., Ferrari-Toniolo, M., Roth, & Tapia, M. 1986, *A&A* 170, 97
- Pismis, P. 1959, *Bol. Obs. Tonantzintla y Tacubaya* 2, No. 18, p37
- Seaton, M.J. 1979, *MNRAS* 187, 73P
- Vacca, W.D., Garmany, C.D., & Shull, J.M., 1996, *ApJ* 460, 914
- Walborn, N.R., Howarth, I.D., Lennon, D.J., Massey, P., Oey, M. S., Moffat, A.F.J., Skalkowski, G., Morrell, N.I., Drissen, L., & Parker, J. W., 2002, *AJ* 123, 2754